A Comparative Analysis of Spatial Multiplexing Techniques for Outdoor MIMO-OFDM Systems With a Limited Feedback Constraint

Stefano Savazzi, *Student Member, IEEE*, Monica Nicoli, *Member, IEEE*, and Mikael Sternad, *Senior Member, IEEE*

***Abstract*—In this paper, we analyze spatial multiplexing techniques for the downlink of a multiple-input–multiple-output (MIMO) orthogonal frequency-division multiplexing (OFDM) system. Our study is focused on outdoor environments characterized by a moderate angular spread. We consider two techniques that are able to separate the downlink data streams associated with different users and to guarantee a fixed error probability by exploiting limited feedback from each user. The grid of beams (GoBs) and the proposed adaptive GoB (AGoB) differ in the way the precoders are designed (by adaptive or fixed processing) and in their scheduling policy. The new AGoB is able to harness partial knowledge of the downlink channel spatial structure to better select the users and adjust their precoders for downlink transmission. The performances of GoB and AGoB are compared in this paper in terms of throughput and cell coverage capability. The radio interface is adapted to fit the requirements for the adaptive modulation and coding with advanced antenna system (AMC-AAS) mode of the IEEE 802.16-2005 standard. Numerical results show that, as long as the channel exhibits a limited angular spread at the base station, the AGoB technique is able to provide significant throughput gains compared with the fixed GoB approach. On the other hand, large angular spreads are proved to have a substantial impact on system performance as the benefits of adaptation are significantly reduced.**

***Index Terms*—MIMO-OFDM systems, multiuser diversity, spatial multiplexing, zero-forcing beamforming.**

I. Introduction

NEXT-GENERATION mobile communication systems are expected to place stringent demands for high quality and high data rates over mobile radio channels. Recent studies on multiple-input–multiple-output (MIMO) antenna systems with orthogonal frequency-division multiplexing (OFDM) signaling have shown that spatial–frequency parallel processing at the transmitter and receiver, combined with fast adaptive transmission, is able to provide significant increases in spectral efficiency [1].

Motivated by capacity analysis of MIMO transmission in single-user scenarios [2], the study of multiuser MIMO systems has recently become crucial for applications where multiple users have to be simultaneously served by a single base station (BS), thus generating multiuser interference (MUI) [3].

In multiuser systems, a traditional time-division multiple-access (TDMA) scheme may be used by the BS to serve one user at a time selected as the one with the best channel condition. Still, this strategy is known to be suboptimal as the multiplexing gain that can be achieved by simultaneous transmission to multiple users is not exploited [4]. The capacity for the multiuser MIMO channel has been analyzed from an information-theoretic viewpoint in [5] by assuming that the transmitter perfectly knows the interfering signals.

Within the class of linear processing techniques for multiuser transmission, space-division multiple-access (SDMA) consists of simultaneously serving multiple users by separate spatial precoding (e.g., beamforming) of each stream. Intracell bandwidth reuse is thus accomplished by creating spatially multiplexed channels [6] that can be associated with different users competing for the same network resource (i.e., for the same time slots and subcarriers, in the OFDM case). Compared with the optimal solution [5], spatial multiplexing is known to be a simpler method that exploits the high spectral efficiency offered by MIMO systems; it provides higher multiplexing gains with respect to traditional TDMA schemes (e.g., space–time coding), but it is very sensitive to the choice of the coding strategy (i.e., the beamforming weights) and to the amount of the available channel state information (CSI) of the links toward the receivers. To provide the necessary robustness to channel fading and MUI, linear precoding should therefore be based on the knowledge of the CSI that can be provided by each receiver using a feedback channel. An optimal solution to the precoding problem with perfect CSI at the transmitter has been proposed in [7], where it is shown how to set up interference-free spatially multiplexed channels by proper design of the precoding matrices or vectors.

This paper focuses on SDMA techniques for outdoor environments, where the BS is located higher than the surrounding scattering (as for cellular systems). Low-complexity precoding techniques are designed to cope with a feedback channel of limited bandwidth that constrains partial (and quantized) CSI at the transmitter [8]. In particular, the downlink of a multiuser frequency-division duplex (FDD) MIMO-OFDM system (or

Manuscript received May 2, 2007; revised December 21, 2007 and February 17, 2008. This work was supported in part by the Ministero dell'Università e della Ricerca–Fondo per gli Investimenti della Ricerca di Base (MIUR–FIRB) Integrated System for Emergency (InSyEme) Project under Grant RBIP063BPH. This paper was presented in part at the IEEE International Conference on Communications, Istanbul, Turkey, June 11–15, 2006. The review of this paper was coordinated by Prof. W. Su.

S. Savazzi and M. Nicoli are with the Dipartimento di Elettronica e Informazione, Politecnico di Milano, 20133 Milano, Italy (e-mail: savazzi@elet.polimi.it; nicoli@elet.polimi.it).

M. Sternad is with the Signals and Systems Laboratory, Department of Engineering Sciences, Uppsala University, 751 21 Uppsala, Sweden (e-mail: ms@signal.uu.se).

Digital Object Identifier 10.1109/TVT.2008.920474

MIMO broadcast channel) conforming to the IEEE 802.16-2005 standard [9], [10] is investigated, with adaptive modulation and coding (AMC) transmission. Such a scheme uses adjacent subcarriers to form subchannels allocated to different users. In addition, the advanced antenna system (AAS) option of the IEEE 802.16-2005 standard is adopted to enable the use of multiple antennas at both the transmitter and the receiver for SDMA, at the price of an increased number of pilots.

A. Related Works

In FDD systems, CSI needs to be delivered to the BS through a feedback channel of limited bandwidth. Performance analysis of spatial multiplexing in realistic conditions should therefore include the effects of partial or quantized CSI. When the feedback is severely limited, important issues are how to quantize the information (the channel gains) needed at the transmitter and how many bits of feedback are required to achieve the desired performances in terms of spectral efficiency or error rate [11], [12].

Linear beamforming techniques based on partial CSI in MIMO broadcast channels are commonly divided into two classes. The *fixed beamforming* based transmission consists of designing predetermined and fixed beamforming vectors (random [13] or optimized [14], [15]) that are associated with each user based on feedback information. On the other hand, the *adaptive beamforming* approach consists of adaptively adjusting the beamforming weights to minimize the MUI experienced by each user. Precoding vectors are thus designed based on information of the interference configuration that is conveyed through the feedback channel. The most commonly used linear adaptive techniques are zero-forcing beamforming (ZFBF) and minimum mean square error beamforming [7], [16], [17], where the first technique is known to be simpler as it does not need the estimation of the noise power and is appropriate when interuser interference is dominant [19], [20].

By reducing frequency-selective channels into an equivalent set of frequency-flat subchannels, OFDM signaling has emerged as an effective solution to combat intersymbol interference caused by wireless multipath fading channel [18]. Orthogonal frequency-division multiple-access (OFDMA) systems add more degrees of freedom in beamforming design as they allow the allocation of different sets of subchannels (or subcarriers) to different sets of terminals, whereas users allocated for the same frequencies can be separated by means of spatial processing. Typical settings [9], [10] prescribe a specific time–frequency resource unit (that consists of a number of adjacent OFDM subcarriers and time slots) that is allocated to the most favorable subset of users based on the available CSI to minimize MUI and maximize the overall throughput [21], [22]. The joint exploitation of beamforming and OFDM processing, together with the availability of a large number of users that are competing for the same communication resource, gives increasing chances to schedule spatially separated users in parallel. As a consequence, designing scheduling algorithms to optimally select the users to be allocated for the same transmission resource is of fundamental importance to fully benefit from multiuser diversity [13]–[20].

In outdoor propagation environments, the BS is typically positioned higher than the surrounding scatterers so that the transmitted signals propagate through a multipath channel with a moderate angular spread [23], [24]. In this case, the fading that impairs the channels to different users is often spatially correlated so that scheduling algorithms can be designed to efficiently arrange the users into groups (or clusters). These subsets are used to separate the users that are allowed to share the same transmission resources from those that must be served in different time or frequency units. Previous studies [25] focused on the uplink case and suggested clustering of users based on their mutual spatial correlation, or, alternatively, on their main direction of arrival (DOA) in the case of moderate angular spread at the BS. In [26], a tree-based scheduling algorithm is proposed to make use of perfect CSI at the transmitter and to organize an arbitrary number of users into groups based on their spatial channel properties.

B. Paper Organization and Main Contributions

In this paper, two SDMA linear precoding strategies are investigated and compared for downlink FDD transmission.

The first strategy, which is referred to as grid of beams (GoB) (see [27, D2.7]), employs a set of *fixed* (predetermined) beamforming precoders (beams) that are switched in time: each mobile station (MS) chooses the best precoder as the one that maximizes the signal-to-noise-plus-interference ratio (SINR) (computed at the output of the beamformer at the receiving antenna array) and conveys this information to the BS by using a limited feedback rate channel. A simple user subset selection algorithm is then employed to find the user group with the highest sum-throughput (the sum of achievable spectral efficiencies for each spatially multiplexed channel).

Second, an alternative, more flexible, approach, which is referred to as *adaptive* GoB (AGoB), is proposed. Differently from GoB, adaptation is now introduced in both user subset selection and precoder computation. User subset selection results as a tradeoff between maximizing the sum throughput and minimizing the mutual spatial correlation among the users' channels; this correlation is evaluated from feedback quantized measures of the main directions of departure (DODs) of the downlink signals. ZFBF is used for precoder computation based on the feedback spatial channel features.

The relative benefits of *adaptive* versus *fixed* beamforming are herein investigated in outdoor environments, where the multipath channel experiences an angular spread [23] that might range from small to larger values.[1] A performance comparison between fixed (GoB) and adaptive (AGoB) spatial multiplexing techniques is performed under varying propagation conditions. For both approaches, the optimum minimum variance distortionless response (MVDR) linear filter [29] is adopted at the receiving side, whereas the modulation and coding parameters are selected based on the SINR at the output of the MVDR filter to satisfy a given bit-error-rate (BER) requirement (as prescribed in the IEEE 802.16-2005 standard [9], [10]). We show that as long as the channel exhibits a limited angular

[1] Angular spreads in outdoor environments typically do not exceed 40° to 50°, with common values ranging between 10° and 30° [24].

spread at the base station (as for outdoor environments [24]), adaptation of user subset and precoders is able to provide significant throughput gains compared to the fixed strategy. On the other hand, simulation results prove that the benefits of adaptation vanish for large angular spreads.

The paper is organized as follows: After the definition of the system and the channel model in Sections II and III, the GoB spatial multiplexing solution is recalled in Section IV. Section V deals with the proposed structure for the BS and MS processing according to the AGoB solution. A performance analysis is carried out in Section VI for both the AGoB and the GoB methods for varying spatial channel conditions. The performance of opportunistic random beamforming [13] is introduced as a reference. The impact of the considered scheduling solutions on the cell coverage is also investigated.

II. System Model

We consider the downlink channel of a multiuser MIMO-OFDMA wireless system, where L active MSs share the same cell. The BS is equipped with a uniform antenna array with N_T Δ_T-spaced elements, whereas each MS has N_R Δ_R-spaced receiving antennas ($N_R \leq N_T$). FDD is used to separate uplink and downlink communications.

In the system under study, multiple access is handled by a combination of time, frequency, and space division. As shown in Fig. 2, the OFDM channel is indeed organized in time–frequency resource units, each consisting of a frame of W subsequent slots (or bursts) of D OFDM symbols and a frequency bin (or subchannel) of B adjacent Δf-spaced subcarriers. The same time–frequency unit is allocated to a subset $\mathcal{S}$ of $M \leq N_T$ users separated by means of spatial multiplexing. The setting under consideration can be equivalently adapted to fit the radio interface requirements for the IEEE 802.16-2005 standard [9], [10], where the AMC mode assigns a modulation and coding scheme per time–frequency unit, and it can also be used in conjunction with multiple antennas at the transmitter and the receiver (AAS option).

We assume that channel estimation (or prediction [35], [36]) can be performed by each user from pilot subcarriers (or preambles) included in each slot, as indicated in Fig. 2. Notice that this feature is available for the AMC mode (with AAS option) of the IEEE 802.16-2005 standard [9], [10].

As shown in Fig. 1, a scheduler at the BS chooses the best subset $\mathcal{S}$ of M users and assigns to them M spatially separated channels by means of M precoding vectors $\{\mathbf{w}_m\}_{m=1}^{M}$. User selection is performed in each time–frequency unit based on some channel measurements drawn by the MS during a previous training phase and transmitted to the BS through a feedback channel.

In any given time–frequency unit, the $N_R \times 1$ signal received by the kth user ($k = 1, \ldots, M$) on a single subcarrier and within a single OFDM symbol can be modeled as

$$\mathbf{y}_k = \sqrt{P_k}\underbrace{\mathbf{H}_k\mathbf{w}_k}_{\mathbf{h}_{kk}}c_k + \sum_{m=1,\, m\neq k}^{M}\sqrt{P_m}\underbrace{\mathbf{H}_k\mathbf{w}_m}_{\mathbf{h}_{km}}c_m + \mathbf{n}_k \quad (1)$$

where for the kth user, $\mathbf{H}_k$ denotes the $N_R \times N_T$ channel matrix, $\mathbf{w}_k$ is the $N_T \times 1$ precoding vector, P_k is the transmitted power, and $c_k \in \mathcal{C}^{(n)}$ is the transmitted symbol with $E[|c_k|^2] = 1$. Adaptive transmission is used, and it is adjusted to attain a fixed BER target (BER $= 10^{-6}$ from Table I). The complex symbol c_k can belong to any of the N available modulation sets $\{\mathcal{C}^{(n)}\}_{n=1}^{N}$ (e.g., according to the IEEE 802.16-2005 standard [9], [10]). Furthermore, the additive noise $\mathbf{n}_k$ is assumed to be zero-mean white complex Gaussian with $E[\mathbf{n}_k\mathbf{n}_k^H] = \sigma^2\mathbf{I}_{N_R}$. In (1), we defined as $\mathbf{h}_{km} = \mathbf{H}_k\mathbf{w}_m$ the $N_R \times 1$ equivalent single-input–multiple-output (SIMO) channel between the BS and the kth MS when the transmitted signal is precoded by $\mathbf{w}_m$. The channel response is herein considered as frequency flat within the frequency bin; thus, the bin size (the number B of adjacent subcarriers; see Fig. 2) needs to be adequately designed according to the specific propagation environment [31].

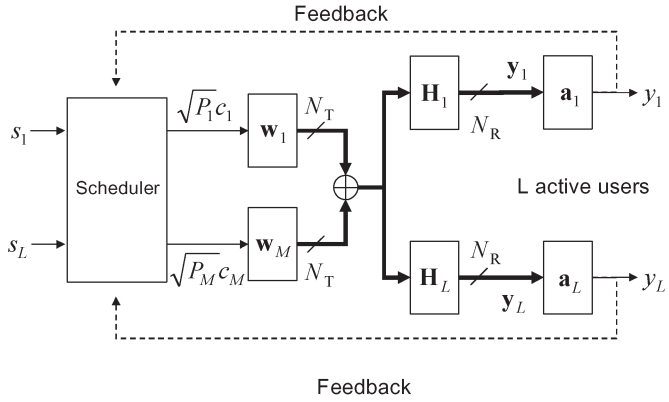

Fig. 1. Downlink multiuser MIMO system.

TABLE I
IEEE 802.16-2005 Transmission Modes and Required SNR Ranges (Over Additive White Gaussian Noise Channels)

Modulation	Coding rate	SNR ρ [dB]	Efficiency γ [bit/carrier]
QPSK	1/2	9.4-11.2	1
QPSK	3/4	11.2-16.4	1.5
16-QAM	1/2	16.4-18.2	2
16-QAM	3/4	18.2-22.7	3
64-QAM	1/2	18.2-22.7	3
64-QAM	2/3	22.7-24.4	4
64-QAM	3/4	>24.4	4.5

As shown in Fig. 1, MVDR spatial filtering $y_k = \mathbf{a}_k^H\mathbf{y}_k$ is performed at the receiver side on the signal (1) to maximize the SINR [29], i.e.,

$$\mathbf{a}_k = \frac{1}{\sqrt{P_k}} \times \frac{\mathbf{Q}_M^{-1}\mathbf{h}_{kk}}{\mathbf{h}_{kk}^H\mathbf{Q}_M^{-1}\mathbf{h}_{kk}}. \quad (2)$$

Here, $\mathbf{Q}_M = \sum_{m=1,m\neq k}^{M} P_m\mathbf{h}_{km}\mathbf{h}_{km}^H + \sigma^2\mathbf{I}_{N_R}$ denotes the noise-plus-interference spatial covariance at the kth MS. This beamforming technique is known to minimize interference under the constraint of a distortionless response to the desired channel (i.e., $\mathbf{a}_k^H\mathbf{h}_{kk} = 1$). CSI is required not only at the MS for the evaluation of the MVDR filter but at the BS as well (in the form of partial or quantized information) for scheduling purposes. For all the considered schemes, specific training phases are carried out to estimate the required parameters.

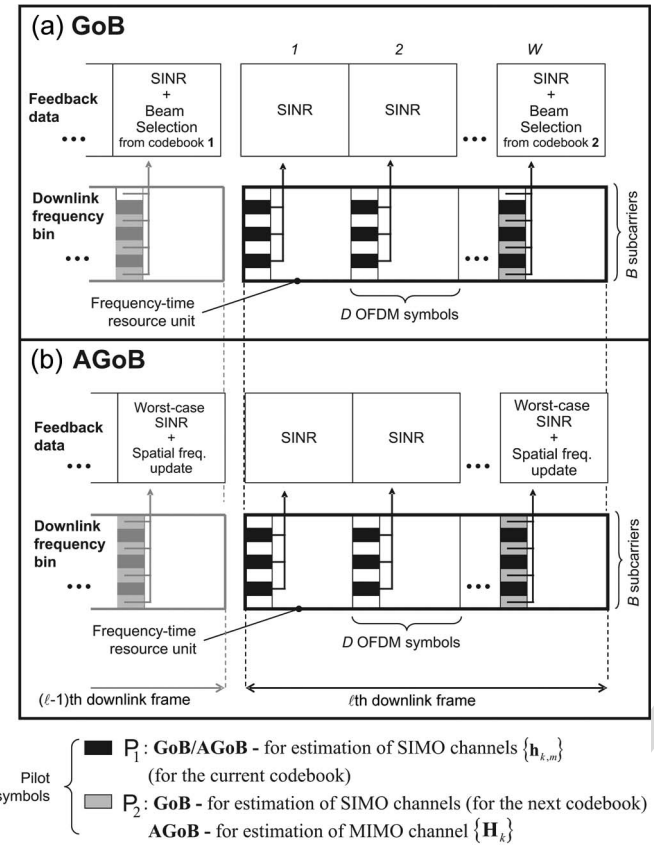

Fig. 2. Overview of the uplink feedback quantities and the downlink frame structure for the (top) GoB scheme and (bottom) AGoB strategy.

With regard to the CSI at the BS, optimum selection of the user set $\mathcal{S}$ and, if necessary, of the corresponding precoding set $\{\mathbf{w}_m\}_{m=1}^M$ (in case AGoB is employed) would require the knowledge of all the MIMO channels $\{\mathbf{H}_m\}_{m=1}^M$ and the consequent intensive feedback transmission. To limit the feedback rate, in this paper, the channel quality information to be evaluated at each MS is reduced to an SINR value ρ_k

$$\rho_k = \frac{P_k \left|\mathbf{a}_k^H \mathbf{h}_{kk}\right|^2}{\sum_{m=1, m\neq k}^{M} P_m \left|\mathbf{a}_k^H \mathbf{h}_{km}\right|^2 + \sigma^2 \mathbf{a}_k^H \mathbf{a}_k} \tag{3}$$

that has to be fed back for each time–frequency resource. Since an MVDR beamformer is employed at each MS, the SINR (3) reduces to the following expression:

$$\rho_k = P_k \mathbf{h}_{kk}^H \mathbf{Q}_M^{-1} \mathbf{h}_{kk}. \tag{4}$$

Notice that each SINR value needs to be quantized before transmission. The number of quantization levels shall be at least equal to the number of allowed transmission modes (i.e., the modulation–coding sets $\mathcal{C}^{(n)}$).

In conjunction with the SINR value, additional feedback is required to help the BS decide the best subset of users to be allocated. The required quantity depends on the specific multiplexing technique (see Section IV for the fixed technique, i.e., GoB, and Section V for the adaptive technique, i.e., AGoB). As a brief outline, for GoB, at least $\lceil \log_2 M \rceil$ bits are required for each user to identify the best precoder among the set $\{\mathbf{w}_m\}_{m=1}^M$; for AGoB, since the precoder needs to be adapted to the user channel, the quantized information related to the main DOD has to be fed back to the BS (see also Fig. 2). With regard the power allocation, in this paper, we restrict our attention to a simplified scheduling system with uniform power assignment, i.e., $P_1 = P_2 = \ldots = P_M$, for both the training and the data transmission phases.

III. Channel Structure

Assume the kth MS, for $k = 1, \ldots, L$, to be sufficiently far away from the BS so that the Kronecker model holds [32]. The $N_R \times N_T$ MIMO channel matrix $\mathbf{H}_k$ can be described as

$$\mathbf{H}_k = \sum_{n=1}^{P} c_{k,n} \mathbf{a}_R(\varphi_{k,n}) \mathbf{a}_T^T(\alpha_{k,n}) \tag{5}$$

which is the superposition of P independent paths (generated from P scatterers) having DOD $\alpha_{k,n}$ and DOA $\varphi_{k,n}$, for $n = 1, \ldots, P$. The $N_T \times 1$ vector $\mathbf{a}_T(\alpha_{k,n})$ denotes the response of the BS antenna array to the DOD $\alpha_{k,n}$; its ith element, $i = 1, \ldots, N_T$, is $[\mathbf{a}_T(\alpha_{k,n})]_i = \exp[-j2\pi/\lambda(i-1)\Delta_T \cos(\alpha_{k,n})]$, where Δ_T is the antenna spacing, and λ is the carrier wavelength. Similarly, the $N_R \times 1$ vector $\mathbf{a}_R(\varphi_{k,n})$ represents the response of the MS antenna array to the DOA $\varphi_{k,n}$, with $[\mathbf{a}_R(\varphi_{k,n})]_i = \exp[-j2\pi/\lambda(i-1)\Delta_R \cos(\varphi_{k,n})]$, and Δ_R denoting the antenna spacing at the MS. The complex fading term $c_{k,n} \sim CN(0, \sigma_{k,n}^2)$ accounts for the amplitude and phase shifts of the wave scattered by the nth scatterer toward the kth MS. According to the wide-sense stationary uncorrelated scattering model for propagation, the fading terms are assumed to be uncorrelated with each other, i.e., $E[c_{k,d} c_{k,n}^*] = 0 \; \forall d \neq n$.

Based on the aforementioned assumptions, the spatial correlation matrices for the signals at the BS ($\mathbf{R}_{T,k}$) and MS ($\mathbf{R}_{R,k}$) arrays, respectively, are

$$\begin{aligned} \mathbf{R}_{T,k} &= \frac{1}{N_R} E\left[\mathbf{H}_k^H \mathbf{H}_k\right] \\ &= \sum_{n=1}^{P} \sigma_{k,n}^2 \mathbf{a}_T^*(\alpha_{k,n}) \mathbf{a}_T^T(\alpha_{k,n}) \end{aligned} \tag{6}$$

$$\begin{aligned} \mathbf{R}_{R,k} &= \frac{1}{N_T} E\left[\mathbf{H}_k \mathbf{H}_k^H\right] \\ &= \sum_{n=1}^{P} \sigma_{k,n}^2 \mathbf{a}_R(\varphi_{k,n}) \mathbf{a}_R^H(\varphi_{k,n}). \end{aligned} \tag{7}$$

Notice that (6) depends only on the DODs from the local scatterers around the terminal, whereas (7) relies on the DOAs.

As a model for the channel spatial correlation matrices, we adopt the propagation layout introduced in [24], as briefly recalled in the following. As depicted in Fig. 3, the MS antenna array is assumed to be surrounded by a ring of uniformly distributed scatterers of radius r_k, with equal mean powers $\sigma_{k,n}^2 = 1/P$. On the contrary, the BS, at a distance $d_k \gg r_k$ from the MS, is not surrounded by any local scatterer (this assumption is generally valid in cellular systems, as the BS

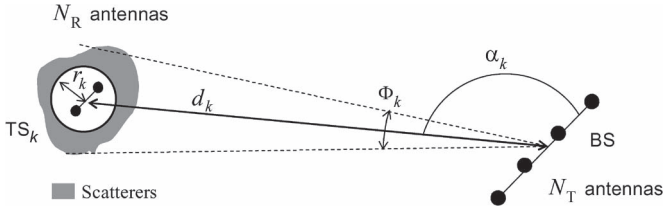

Fig. 3. Spatial structure of the downlink channel.

position is high compared to the average ground level). It follows that the signal to the kth MS is characterized by the angular spread $\Phi_k \simeq 2r_k/d_k$ around a main DOD, which is denoted here by α_k. The DOD spread Φ_k will generally be smaller than the beamwidth of the BS array. Under such conditions, for $P \to \infty$, the MIMO channel correlation matrices (6) and (7) assume a simplified expression that has been derived in [24]. In particular, the correlation of the signals from the pth and qth transmitting antennas ($p, q = 1, \ldots, N_T$) is therein shown to be

$$\lim_{P\to\infty}[\mathbf{R}_{T,k}]_{pq} = \exp\left[j\frac{2\pi}{\lambda}(p-q)\Delta_T\cos(\alpha_k)\right] \times I_0\left(\frac{2\pi}{\lambda}\Delta_T(p-q)\Phi_k\sin(\alpha_k)\right) \quad (8)$$

where $I_0(\cdot)$ is the zeroth-order modified Bessel function of the first kind. By appropriately adjusting the angular spread Φ_k in (8), a propagation environment with either moderate (small Φ_k) or rich (large Φ_k) scattering can be modeled.

IV. Overview of the Fixed GoB

Fixed beams for SDMA can be seen as an extension of the cellular structure with reuse of frequencies [27]: to increase the throughput, spatial reuse of beams is employed using beam selection information fed back by each user together with an SINR value calculated according to (4). The M-precoder set (or codebook) $\{\mathbf{w}_m\}_{m=1}^M$ is chosen among a group of K predetermined fixed codebooks. To provide full coverage (for a uniform distribution of users over the cell), codebook selection is done on a frame-by-frame basis so that all the K available codebooks are selected during K subsequent frames.

Fig. 4 shows the design of precoders (or beams) proposed in [27] for a scheme with $K = 2$ codebooks: herein, the beampattern is plotted versus the main DOD α_k of the signal from the BS, for a transmitting array of $N_T = 4$ antennas. A simple heuristic rule can be given to minimize MUI: only nonneighboring beams form a codebook (e.g., in Fig. 4, beams $\{1, 3, 5\}$ form codebook 1, whereas beams $\{2, 4, 6\}$ form codebook 2); users allocated to the M beams of a given codebook can share the same time–frequency resource ($M = 3$ in the example of Fig. 4). Assuming an antenna array aperture of 120° at the BS, $K = 2$ codebooks span the whole BS aperture, and they can be switched from frame to frame to cover the whole cell. Chebychev tapering is proposed in [27] to optimize the shape

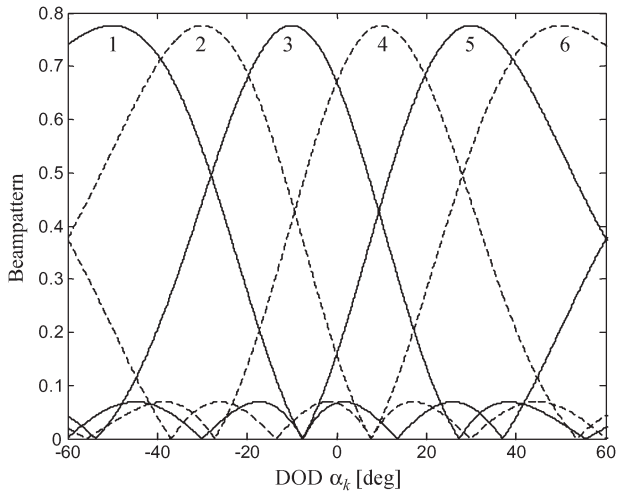

Fig. 4. Beampattern from six equispaced Chebychev tapered beams.

of the beams; sidelobe suppression of 21 dB is adopted in this paper according to the scheme therein proposed.[2]

At the receiving front end, each user has the knowledge of the transmitted codebook, so that optimal beam selection can be carried out at each MS by maximizing the SINR (4) at the output of the MVDR filter. As indicated in Fig. 2, to allow for the SINR evaluation, a specific training phase (indicated by $\mathcal{P}_1$) needs to be carried out in each slot by separately activating at the BS the M precoders of the current codebook, i.e., $\{\mathbf{w}_m\}_{m=1}^M$, and estimating at each MS the whole set $\{\mathbf{h}_{km}\}_{m=1}^M$ of M precoded channels. Using the M estimated channels, the kth MS can then evaluate the M SINR values that correspond to the M possible selections of the precoder $\mathbf{w}_k$. Each SINR value is derived from (4) by using one of the estimated beams as $\mathbf{h}_{kk}$ and the remaining $M-1$ beams as the interfering set $\{\mathbf{h}_{km}\}_{m\neq k}$. The optimal precoder for the kth MS is then selected as the one that yields the maximum SINR. Such beam selection information has to be fed back to the BS (e.g., using $\lceil \log_2(M) \rceil$ bits), together with the corresponding maximum SINR value, before beginning the downlink frame. A second kind of training phase (indicated by $\mathcal{P}_2$ in Fig. 2) is carried out in the last burst of each frame to allow for a new user subset selection that is maintained during the next frame. Similarly as before, this is done by activating at the BS the M precoders of the codebook that is chosen for the upcoming frame (which is different from the current frame) and by estimating at each MS the new set of M precoded channels, and thus the SINRs, to perform a new beam selection.

The scheduling procedure based on these feedback measurements consists of two distinct phases.

1) **Beam allocation.** The user subset $\mathcal{S}$ (recall that precoders are predetermined and maintained during the whole frame) is selected by the scheduler for a specific time–frequency unit according to the measurements that are fed back by each user, i.e., the beam selection

[2]The use of Chebychev tapered beamforming weights is primarily motivated by practical constraints. Optimal fixed precoders shall generally depend on the particular environment (see, for example, the Grassmannian beamforming solution [14] for the independent identically distributed Rayleigh fading case and [28] the correlated Rayleigh fading case).

information and the corresponding SINR value. The optimal subset of M users is then found by grouping users with different precoders and by choosing the group that maximizes the throughput. Other optimization metrics that cope with fairness aspects might also be taken into account.

2) **Transmission mode selection.** The SINR information is updated over each slot by the MS (to account for possible channel variations), and it is used by the BS to design and update the transmission modes to be associated with each selected terminal.

Notice that both GoB and AGoB require each beamforming weight to be computed in hardware that is limited by finite resolution and calibration errors [30].

V. AGoB

Here, a novel *adaptive* version of the fixed GoB approach [27] is proposed. As compared to GoB, by allowing a limited increase in the feedback rate and in the number of pilot subcarriers for each slot (see Fig. 2), the method is able to adapt the design of the beamforming vectors and of the user subset to the spatial structure of the users' channels based on quantized CSI.

The training phase $\mathcal{P}_1$ remains unaltered compared to GoB, whereas $\mathcal{P}_2$ (that in GoB was used to estimate the SIMO channels for the next codebook) is now exploited to draw information about the DODs of the downlink signals to adapt scheduling and precoding to the spatial channels' structure. Differently from GoB, the training procedure $\mathcal{P}_2$ is carried out without the use of precoding to allow the estimation of the MIMO channel matrix $\mathbf{H}_k$ at the kth MS. The number of pilot symbols for the estimation of $\mathbf{H}_k$ is typically larger than that required to estimate the SIMO channels $\{\mathbf{h}_{km}\}_{m=1}^{M}$ in GoB. Moreover, if the number of antennas is moderate, this difference can be regarded as negligible.

The MIMO channel is used by the kth MS to evaluate the spatial correlation matrix $\mathbf{R}_{T,k}$[3] and to estimate the spatial frequency $f_k = \cos(\alpha_k)$ associated to the main DOD α_k (see Section V-A). Additional information to be evaluated at the MS is a lower bound $\hat{\rho}_k$ for the SINR (4) based on a worst-case choice of the interference configuration[4] (see Section V-C). Both measurements, i.e., $\hat{f}_k$ and $\hat{\rho}_k$, are quantized and transmitted on the feedback channel. The feedback rate clearly depends on the velocity of the variations of the second-order channel statistics (i.e., the matrix $\mathbf{R}_{T,k}$) and, thus, on the degree of MS mobility.

The scheduling procedure based on the aforementioned measurements consists of two phases.

1) **Spatial channel allocation.** The user subset $\mathcal{S}$, as well as the precoders $\{\mathbf{w}_k\}_{k=1}^{M}$ to be maintained during the whole frame, are selected by the scheduler according to the feedback measurements $\hat{\rho}_k$ and $\hat{f}_k$. Based on the SINRs $\hat{\rho}_k$, a suboptimal choice of the transmission modes is also carried out by using the mapping scheme in Table I. ZF-based beamformers are designed at the BS based on $\hat{f}_k$; the pilot symbols $\mathcal{P}_1$ are then transmitted to the chosen terminals using these precoders (see Fig. 2).
2) **Transmission mode selection.** Once the precoded channels $\{\mathbf{h}_{km}\}_{m=1}^{M}$ have been estimated by the selected terminals from the pilot symbols $\mathcal{P}_1$, the real SINR measurements $\{\rho_k\}_{k=1}^{M}$ can be evaluated from (4) and be fed back (after quantization) for each slot. Transmission mode decisions are then updated by the scheduler according to the new SINR measurements and are valid for the remaining $W-1$ bursts. This aspect will be further analyzed in Section VI-A.

A. Spatial Frequency Estimation

From (8), under the condition of a limited angular spread ($\Phi_k \simeq 0$) such that $I_0(2\pi/\lambda\Delta_T(p-q)\Phi_k\sin(\alpha_k)) \approx 1$, the elements of the spatial correlation matrix $\mathbf{R}_{T,k}$ reduce to

$$[\mathbf{R}_{T,k}]_{pq} \approx \exp\left[j\frac{2\pi}{\lambda}(p-q)\Delta_T\cos(\alpha_k)\right]$$

for $p, q = 1, \ldots, N_T$, and $k = 1, \ldots, L$. The spatial correlation structure at the transmitting array can thus be approximated by the rank-1 matrix (see Appendix A)

$$\mathbf{R}_{T,k} \approx \mathbf{a}_T^*(\alpha_k)\mathbf{a}_T^T(\alpha_k) = \mathbf{b}(f_k)\mathbf{b}^H(f_k)$$

where the change to the variable f_k has been introduced to simplify the analysis in the remainder of this paper, with $f_k \in [-1, +1]$ as the spatial frequency corresponding to the main DOD α_k and $\mathbf{b}(f_k) = \mathbf{a}_T^*(\alpha_k)$ as the steering vector expressed as a function of the spatial frequency f_k. The main DOD α_k, or equivalently the corresponding spatial frequency f_k, can be estimated at the MS using the spatial correlation matrix $\mathbf{R}_{T,k}$ drawn from the pilots $\mathcal{P}_2$. The problem reduces to solve a rank-1 constrained least-squares optimization

$$\begin{aligned}\hat{f}_k &= \arg\min_f \left\|\mathbf{R}_{T,k} - \mathbf{b}(f)\mathbf{b}^H(f)\right\|^2 \\ &= \arg\max_f \left\{\mathbf{b}^H(f)\mathbf{R}_{T,k}\mathbf{b}(f)\right\} \end{aligned} \quad (9)$$

where $\|\cdot\|$ denotes the Frobenius norm operator.

Once estimated at the MS, the spatial frequency $\hat{f}_k$ needs to be transmitted to the BS for scheduling purposes. Since, in practical systems, DODs can be considered as slowly varying among each time–frequency unit, only a limited feedback rate is actually required for the transmission of $\hat{f}_k$. In particular, since the frame duration is designed according to the fast-fading channel parameters, the spatial frequency has to be estimated during the mobile switching-on phase; then, it may simply be updated every W slots (thus, on every new frame) using a lower number of bits. Appendix B gives further details on how to perform both the estimate and the update in the most efficient and simplest way.

[3]The matrix $\mathbf{R}_{T,k}$ can be estimated or predicted by averaging over a number of channel realizations from different time–frequency units (see Appendix A for further details).

[4]Since the precoders are adaptively designed by the BS (and not known at the MS), the worst-case SINRs $\hat{\rho}_k$ can be only a measure of the *maximum* expected level of interference experienced by each user.

TABLE II
SYSTEM PARAMETERS AND DOWNLINK RADIO INTERFACE
(SEE THE AMC MODE FOR IEEE 802.16-2005 [9], [10])

Number of antennas	$N_T = 4,\ N_R = 2$
Antenna spacings	$\Delta = 0.5\lambda$
Max. number of streams	$M = 3$
Cell sectors	$120\,\mathrm{deg}$
Background SNR	$\mathrm{SNR} = 18\mathrm{dB}$
Minimum spatial separation	$\beta = \sin(20\,\mathrm{deg})$
Maximum terminal velocity	$v = 50\mathrm{km/h}$
Carrier frequency	$f_c = 3.5$ GHz
Available bandwidth	$B_w = 10$ MHz
Subcarrier spacing	$\Delta f = 10.9$ kHz
OFDM symbol period	$102.8\ \mu\mathrm{s}$
Burst (slot [9]) length	$D = 3\ (333\mu\mathrm{s})$
Frequency bin length (9x2 subcarriers)	$B = 18\ (181\mathrm{kHz})$
Frequency bins	$F \leq 48$
Frame length	$W = 4\ (1.2ms)$

B. Scheduling and Precoder Computation

Herein, the focus is on the processing to be carried out at the BS. In particular, both the problem of finding the best user subset $\mathcal{S}$ and how to set up the precoders for a specific set of M feedback spatial frequencies are considered. To minimize the complexity, a suboptimal solution to the scheduling problem is proposed. The transmission modes $\mathcal{C}^{(n)}$ are selected based on the SINR measurements (4) according to the target BER, as exemplified in Table I (from the transmission modes in the IEEE 802.16-2005 standard [9], [10]). We also assume that F scheduler modules are independently operating on the F available frequency bins (see Table II).

1) User Subset Selection: With L users competing for a specific time–frequency resource, the scheduler exploits the feedback SINR lower bounds $\{\hat{\rho}_k\}_{k=1}^{L}$ and the spatial frequencies $\{\hat{f}_k\}_{k=1}^{L}$ to find all sets of M users fulfilling a spatial separation constraint (to avoid critical MUI situations) and, among the selected sets, to find the set that maximizes the whole throughput.

Let $\mathcal{R}_0 = \{\mathcal{S}_i\}_{i=1}^{N_\mathcal{S}}$ indicate the collection of all the $N_\mathcal{S} = L!/(M!(L-M)!)$ subsets of M users that can be obtained from the whole set of L active MSs. For the ith subset, $\mathcal{S}_i = \{k_{i,1}, \ldots, k_{i,M}\}$, the corresponding SINR lower bounds and spatial frequency values will be indicated by $\{\hat{\rho}_{k_{i,1}}, \ldots, \hat{\rho}_{k_{i,M}}\}$ and $\{\hat{f}_{k_{i,1}}, \ldots, \hat{f}_{k_{i,M}}\}$, respectively. For any subset $\mathcal{S}_i$, we define the minimum spatial separation between its users as

$$\mathcal{L}(\mathcal{S}_i) = \min_{k_{i,\ell}, k_{i,m} \in \mathcal{S}_i,\, \ell \neq m} \left| \hat{f}_{k_{i,\ell}} - \hat{f}_{k_{i,m}} \right|. \tag{10}$$

We also define the sum throughput as

$$\gamma(\mathcal{S}_i) = \sum_{m=1}^{M} \gamma(\hat{\rho}_{k_{i,m}}) \tag{11}$$

where $\gamma(\cdot)$ (in bits per payload symbol per user) denotes the maximum spectral efficiency that can be achieved given the SINR value argument, according to Table I. Herein, maximum sum-throughput-based scheduling is employed; nevertheless, the proposed approach could easily be extended in case other throughput measurements or scheduling schemes (such as proportional fair scheduling [33]) are adopted.

From the whole collection of possible subsets $\mathcal{R}_0$, the set $\mathcal{R}_1 \subseteq \mathcal{R}_0$ is generated so that

$$\mathcal{R}_1 = \{\mathcal{S}_i \in \mathcal{R}_0 | \mathcal{L}(\mathcal{S}_i) > \beta\}. \tag{12}$$

This new set $\mathcal{R}_1$ contains all the subsets that fulfill a minimum spatial separation constraint. To avoid critical MUI situations, each selection belonging to $\mathcal{R}_1$ has a spatial separation at least greater than β (which needs to be numerically computed, as shown in Appendix C and Section VI). The next step is to generate a second subset $\mathcal{R}_2$, with $\mathcal{R}_2 \subseteq \mathcal{R}_1$, as shown in the following:

$$\mathcal{R}_2 = \left\{ \mathcal{S}_i \in \arg\max_{\mathcal{S}_i \in \mathcal{R}_1} \gamma(\mathcal{S}_i) \right\}. \tag{13}$$

This is thus obtained by picking all the selections $\mathcal{S}_i \in \mathcal{R}_1$ that have the highest throughput metric $\gamma(\mathcal{S}_i)$ in (11).

If the subset $\mathcal{R}_2$ contains more than one candidate subset,[5] the best user subset $\mathcal{S}$ is finally selected as the user group that maximizes the minimum spatial separation metric $\mathcal{L}(\cdot)$, i.e.,

$$\mathcal{S} = \arg\max_{\mathcal{S}_i \in \mathcal{R}_2} \mathcal{L}(\mathcal{S}_i). \tag{14}$$

This is done to find a subset that provides the maximum value for the sum throughput $\gamma(\mathcal{S}_i)$ (as $\mathcal{S}_i \in \mathcal{R}_2$) and to jointly maximize the angular separation between users (to minimize the mutual interference). As shown in Section VI, a drawback of this approach is that the selected users tend to be clustered with a high probability to specific and fixed regions of the angular cell sector. This aspect might be critical for fixed applications, where uniform cell coverage is required to guarantee fairness.

2) Precoder Computation: Once the set $\mathcal{S}$ is chosen, appropriate precoding vectors have to be set up for the M selected users according to the feedback spatial frequencies $\hat{\mathbf{f}} = [\,\hat{f}_1 \ \cdots \ \hat{f}_M\,]$. Defining as $\mathbf{B}(\hat{\mathbf{f}}) = [\,\mathbf{b}(\hat{f}_1) \ \cdots \ \mathbf{b}(\hat{f}_M)\,]$ the $N_T \times M$ matrix gathering the BS antenna array responses to the M spatial frequencies, the precoding matrix $\mathbf{W}(\mathbf{f}) = [\,\mathbf{w}_1 \ \cdots \ \mathbf{w}_M\,]$ is calculated as

$$\mathbf{W}(\hat{\mathbf{f}}) = \mathbf{B}(\hat{\mathbf{f}}) \left[\mathbf{B}^H(\hat{\mathbf{f}}) \mathbf{B}(\hat{\mathbf{f}}) \right]^{-1}. \tag{15}$$

ZFBF is thus accomplished as in [19]. Notice that this choice makes the mth precoder $\mathbf{w}_m$ orthogonal to all other vectors $\mathbf{b}(\hat{f}_k)$ within $\mathcal{S}$ for $k \neq m$. Therefore, in the ideal case of null angular spread at the BS and for perfect knowledge of each user DOD ($\hat{f}_k = f_k$), this orthogonal precoding leads to null MUI in the MS signal (1); on the other hand, in more realistic propagation conditions that exhibit larger angular spreads, perfect interference rejection is no longer guaranteed.

C. Lower Bound SINR Computation at the MS

During the spatial channel allocation phase, the L active MSs are in charge of sending to the BS a measure of their SINR

[5] Notice that the solution to (13) is likely to be not unique even for small L as the number of allowed transmission modes (with associated spectral efficiencies in Table I) is finite.

value. However, having no knowledge of the M precoders $\{\mathbf{w}_m\}_{m=1}^{M}$ that influence the intercell interference configuration, the MS cannot evaluate the exact SINR value ρ_k from (4). Hence, we propose to feed back from the kth MS a lower bound $\hat{\rho}_k$ corresponding to the worst case of interference configuration. From (12), the worst configuration of interferers for the kth user is associated with the set of β-spaced spatial frequencies $\{f_m^{(k)}\}_{m=1}^{M}$ distributed within the cell sector around the kth value $f_k^{(k)} = \hat{f}_k$.[6] The corresponding precoding vectors $\{\mathbf{w}_m\}_{m=1}^{M}$ can be computed as in (15) from the selected frequencies $\{f_m^{(k)}\}_{m=1}^{M}$. The precoders are then plugged in (4) together with the power values $\{P_k\}_{k=1}^{M} = P/M$, yielding the SINR lower bound $\hat{\rho}_k$.

VI. Performance Comparison and Numerical Results

In this section, a MIMO downlink radio interface is simulated in accordance with the IEEE 802.16-2005 standard [9], [10]. The main system parameters are summarized in Table II. The number of antennas at the BS and MS is $N_T = 4$ and $N_R = 2$, respectively. The minimum angular separation among users is selected as $\beta = \sin(20^\circ)$ according to [34] (see also Appendix C). The basic allocation unit [9], [10] is herein defined through a bin, which is a set of nine contiguous subcarriers observed over a single OFDMA symbol. In this paper, according to the second type of AMC subchannel, a slot is defined as a unit of two bins (i.e., $B = 18$ adjacent subcarriers) by $D = 3$ OFDMA symbols. Since the AMC permutation subcarriers assigned to a particular subchannel do not overlap with those of any other subchannel, for a physical-level simulation, the performance in noise- and interference-limited systems can be completely assessed by restricting our attention to a single time–frequency unit (and subcarrier). Each slot carries $D \cdot B = 54$ symbols; of these symbols, as shown in Fig. 2, at least M should be allocated for the estimation of the precoded channels $\{\mathbf{h}_{ik}\}_{i=1}^{M}$ for the current frame (i.e., the pilots $\mathcal{P}_1$). Other pilots should be available (i.e., the pilots $\mathcal{P}_2$) for the estimation of the MIMO channel matrix $\mathbf{H}_k$ (for AGoB) or for the estimation of the precoded channels for the next frame (for GoB). A number of symbols are also reserved for downlink control messaging and synchronization. At the BS, spectral efficiencies are computed from SINR measurements, as reported in Table I. The number of bits used for spatial frequency feedback is $b = 6$, and a lower number of bits are required during the tracking mode (see Appendix B).[7] For performance assessment, we will assume perfect knowledge of $\{\mathbf{h}_{km}\}_{m=1}^{M}$ and $\mathbf{R}_{T,k}$ at the kth MS (as for a large number of pilot symbols).

The performances of AGoB and fixed GoB are herein evaluated for varying channel conditions and compared with those of the (opportunistic) orthonormal random beamforming approach (ORBF) [13]. This is a nonadaptive scheme as the GoB scheme but is based on randomly chosen orthonormal precoders $\{\mathbf{w}_m\}_{m=1}^{M}$. In other words, the same signal from each antenna is modulated by an independent gain whose phase and magnitude are random and uniformly generated so that each beamformer is orthogonal with the other. As for the GoB scheme, the beam selection information, together with the SINR measurement, is tracked by each user and fed back to the BS to form a basis for scheduling. Compared with beamforming solutions such as GoB and AGoB, this scheme does not need any antenna array calibration.

A. Performance Comparison for GoB, AGoB, and ORBF

In this section, a first performance comparison is carried out for AGoB, GoB, and ORBF. The propagation channel is simulated according to the multipath structure in Section III. More specifically, the fading coefficients in the matrix $\mathbf{H}_k$ are assumed to be Rayleigh distributed, i.e., constant within a frame interval but varying from frame to frame. Temporal variations are simulated according to the Clarke model and approximated by a second-order autoregressive (AR-2) random process [36]. With regard to spatial channel structure, users are placed at a fixed distance from the BS with the main DOD α_k uniformly distributed within the cell sector. Each DOD slowly varies over the frames according to the AR-1 model [37] $\alpha_k(\ell) = \alpha_k(\ell-1) + \xi_k$, where $\xi_k \sim \mathcal{N}(0, \sigma_\alpha^2)$, and $\sigma_\alpha = 0.5^\circ$[8]. Since multipath channels in urban, suburban, and rural macrocells are usually characterized by angular spreads ranging from 10° to 30° [23], [24], herein, we choose a one-sided Gaussian random variable $\Phi_k \sim \mathcal{N}(15^\circ, \sigma_\Phi^2)$ for the angular spread at the BS, with mean 15° and standard deviation $\sigma_\Phi = 5^\circ$ ($\Phi_k \geq 0\ \forall k$).[9] The spatial correlation of the channel gains at the transmitter and the receiver is modeled according to [24].

Fig. 5 shows the spectral efficiency for each scheduled channel (ordered by the SINR value $\hat{\rho}_k$) averaged over user positions, fading channels (frames), and data. Accordingly, Fig. 6 gives the average SINR at the MS after MVDR filtering. Both plots are drawn versus the number L of active users. Since, in most practical cases, the number of active users competing for a specific resource unit has a wide and unpredictable range, we considered L values ranging from $L = 3$ to $L = 12$ to model the cases of either small or large cell loading, respectively. For the evaluation of AGoB spectral efficiency and SINR, we considered a single OFDM payload symbol within each time–frequency unit, which is taken either from the first slot (AGoB—burst 1) or from any of the remaining $W - 1$ slots (AGoB—bursts $2, \ldots, W$) of the downlink frame.

[6] As an example, for $M = 3$ and $\hat{f}_1 = 0$, the two interferers for user 1 are placed at the two spatial frequencies having spatial separation from $\hat{f}_1$ equal to β, i.e., $f_2^{(1)} = \beta$ and $f_3^{(1)} = -\beta$.

[7] Here, the 2^6 available spatial frequencies are chosen to uniformly span the 120° cell sector in the angular domain (other solutions might be employed as well). The resulting maximum quantization error is approximately 1°.

[8] In general, the statistics of the DOD variations shall be related to the propagation environment and to the kinematics of the mobile terminals (e.g., the Doppler frequency). The simplified model used in this section is adopted only to ease the numerical analysis, without affecting the main reasoning of this paper.

[9] For this propagation scenario, we observed that the spatial frequencies can be tracked by sending only 1 bit for the frequency update (tracking mode), with negligible performance degradation. A periodical estimate refresh that uses 6 bits is also needed. The refresh period can last several frames, depending on the spatial frequency variability.

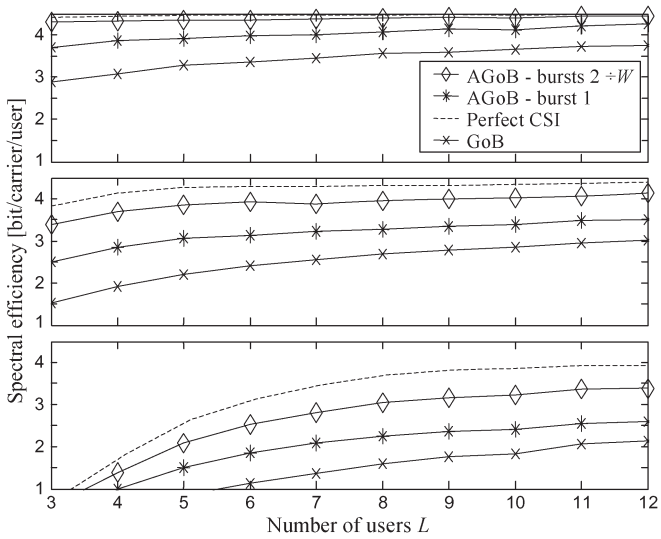

Fig. 5. Average spectral efficiency on each scheduled channel versus the number L of active users for AGoB, GoB, and the interference-free case. For AGoB, the spectral efficiency is evaluated in either the first burst or the remaining $W-1$ bursts in the frame.

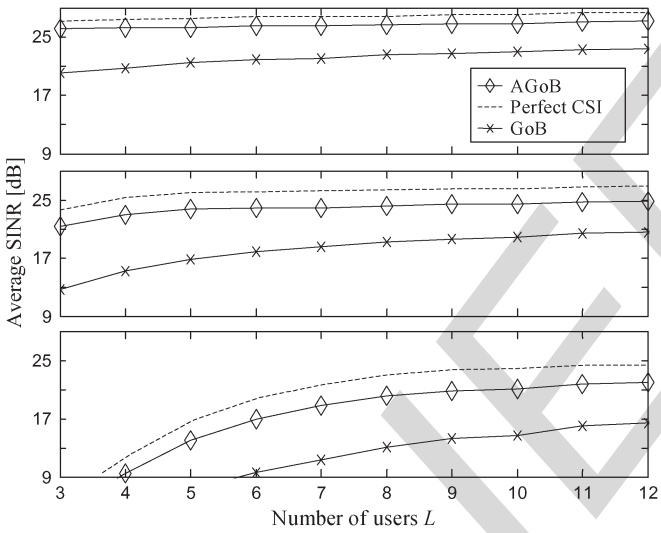

Fig. 6. Average SINR at the MS after MVDR on each scheduled channel versus the number L of active users for AGoB, GoB, and the interference-free case.

As shown in Fig. 5, when considering the first slot, we found that for the considered number of active users L, an average spectral efficiency gain of at least 0.5 bit/carrier/user (or, equivalently, per channel) can be achieved compared with the GoB solution. The gain is doubled (at least 1 bit/carrier/user) in the case of payload symbol placed in any of the remaining $W-1$ bursts. In Fig. 6, we can also conclude that an SINR gain of at least 4 dB can be obtained for each user in any burst of the frame. It is also worth noticing that the performance gains are uniformly distributed among the scheduled channels. Benefits in spectral efficiency and SINR values are more significant when few users are competing for the same resource unit (i.e., for low L).

The MUI reduction capability of the proposed AGoB system can be inferred from both Figs. 5 and 6 through a comparison with the spectral efficiency (Fig. 5) and the SINR (Fig. 6) that

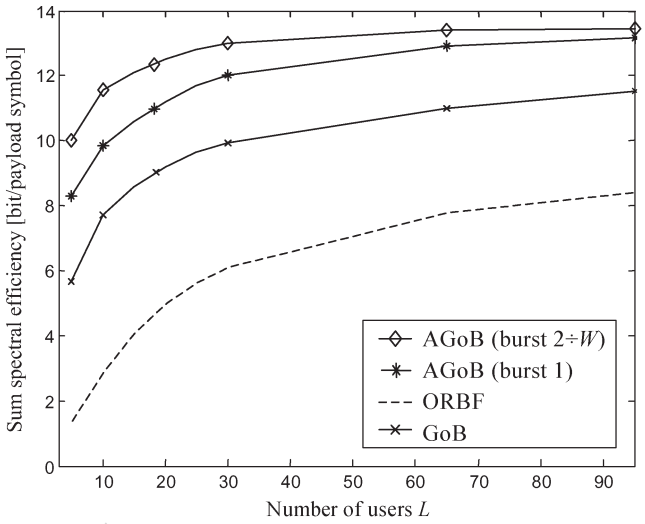

Fig. 7. Average sum spectral efficiency versus the number L of active users for AGoB, GoB, and (dashed line) ORBF. For AGoB, the spectral efficiency is evaluated in either the first burst or the remaining $W-1$ bursts in the frame.

can be achieved when full CSI of each user is available (dashed lines). For this ideal case, the user subset selection is carried out as in [26], where precoders are computed from a zero-forcing technique that exploits perfect knowledge of the users' channel matrices. For a fair comparison with our scheme, one single stream is associated with each user. Notice that since full CSI is available at the BS, each column of the matrix $\mathbf{B}$ in (15) contains the leading right eigenvector for each channel matrix $\mathbf{H}_k$, $k=1,\ldots,M$. Fig. 6 shows that for realistic channel conditions, the SINR loss experienced by AGoB with respect to this ideal case (perfect CSI) is less than 2.5 dB for the considered number of users L.

Under the same spatial channel conditions, Fig. 7 shows the average sum spectral efficiency versus the number L of active users. Here, the AGoB method is also compared with the ORBF case (dashed line). Although the problem of antenna array calibration is avoided by ORBF, significant performance degradation is observed in the case of random beamforming due to the low degree of multiuser diversity offered by the considered multiuser scenario. For the considered setting, a higher number of users (at least $L>40$ users competing for the same time–frequency unit) are indeed required by the random beamforming scheme to reach the same performances as for GoB and AGoB.

From these results, we can conclude that even with partial CSI at the transmitter, the proposed AGoB scheduling and precoding approach at the BS, jointly with MVDR filtering at the MS, is effectively able to reduce MUI, thus increasing the overall spectral efficiency.

B. Impact of the Propagation Environment on the Performance

In this section, the impact of the propagation environment on the system performance is investigated by analyzing the effect of the channel angular spread on the average throughput. The scattering scenario ranges from line of sight (LOS, for a low angular spread Φ_k) to rich scattering (for a large angular spread Φ_k). The corresponding performances are shown in

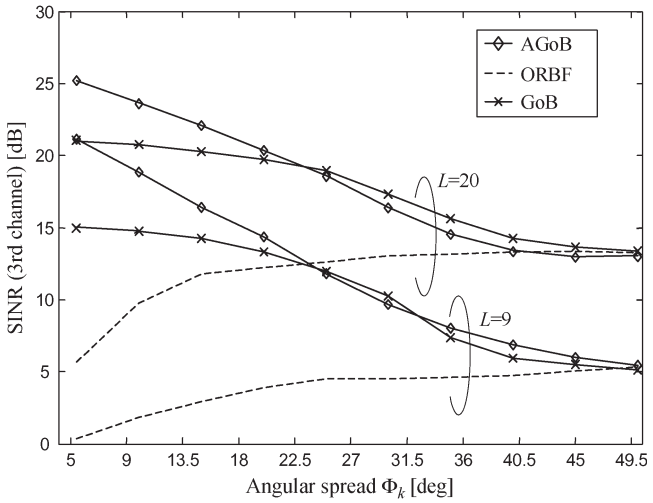

Fig. 8. Average lowest SINR at the output of the scheduler for varying channel conditions and number of active users $L = 9$ or $L = 20$. The angular spread is $\Phi_k \sim N(E[\Phi_k], \sigma^2_\Phi), \Phi_k \geq 0, \sigma_\Phi = 5°$; the average spread $E[\Phi_k]$ ranges from 9° to 48°.

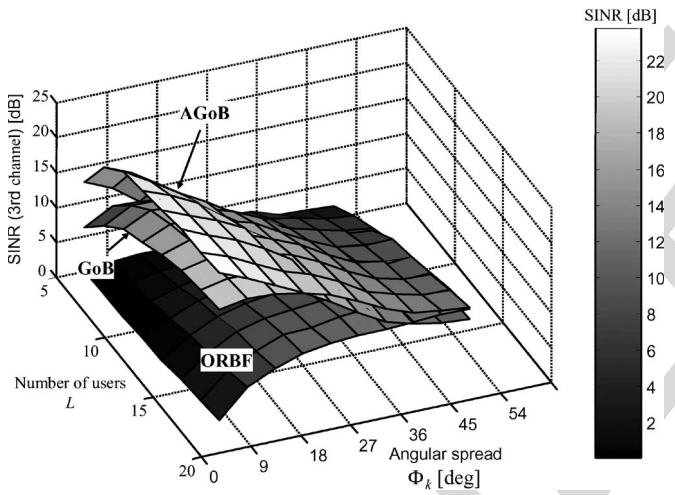

Fig. 9. Average lowest SINR at the output of the scheduler for varying channel conditions (angular spread) and number of active users L ranging from 5 to 20.

Fig. 8 in terms of the (average) lowest SINR at the output of the scheduler for a number of active users $L = 9$ or $L = 20$. We show that a critical threshold angular spread exists, above which the performances of the fixed GoB are similar to those of AGoB. This means that for outdoor environments with large angular spreads, the fixed beamforming solution (GoB) overcomes precoder adaptation (AGoB). In particular, for the considered simulation setting, the threshold angular spread is found to have marginal dependence on the number of users (see also Fig. 9), and it is approximately equal to 25° to 27°. The performances of opportunistic random beamforming (dashed lines in Fig. 8) scale with the angular spread, as expected. For the considered setting, an angular spread of 35° renders $L = 20$ users sufficient to have comparable performances with those of GoB and AGoB.

In Fig. 9, the (average) lowest SINR at the output of the scheduler is plotted versus both the number L of active users and the angular spread Φ_k. As expected, since, in practice, the number of users competing for the same time–frequency unit is limited, the adaptive strategy is shown to be a reasonable candidate for outdoor environments, where multipath propagation is characterized by a moderate angular spread.

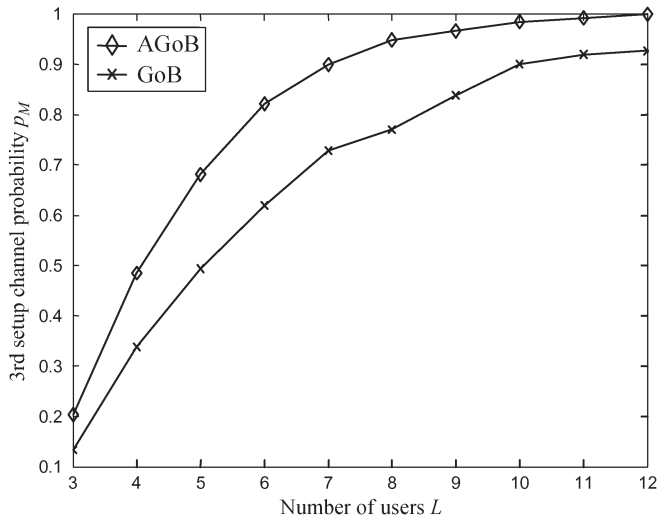

Fig. 10. Third setup channel probability p_M versus the number of users L for AGoB and GoB ($M = 3$).

C. Cell Coverage

In this section, a cell coverage analysis is dealt with under the simplifying assumption that the spatial frequency f_k can be assumed as a reliable measure of the angular position of the kth MS within its cell.[10] A performance comparison is first carried out by analyzing the probability p_M that all the M channels can be reliably set up; this probability is $p_M = \Pr[\gamma(\min_{k\in\mathcal{S}}(\hat{\rho}_k)) \geq 1]$ for AGoB and $p_M = \Pr[\gamma(\min_{k\in\mathcal{S}}(\rho_k)) \geq 1]$ for GoB. It is evaluated in Fig. 10 for both methods, for $M = 3$, and for a varying number L of active users. As before, the angular spread Φ_k at the BS is a one-sided Gaussian random variable $\Phi_k \sim \mathcal{N}(15°, \sigma^2_\Phi)$, $\Phi_k \geq 0$ with mean 15° and standard deviation $\sigma_\Phi = 5°$. Opportunistic random beamforming is not considered in this analysis as its performance was proved to be unsatisfactory in moderate angular spread environments (see the results in Section VI-B). On the other hand, the comparison between AGoB and GoB in Fig. 10 shows that to schedule M users for the same time–frequency unit, the first method requires a total number of MSs that are lower compared with the second approach; for $L = 7$, AGoB guarantees a third channel to be set up with a probability larger than 90%, whereas GoB needs a higher L value to achieve the same reliability (see Fig. 12). We may thus conclude that whenever a moderate number of active users are considered, the AGoB approach can lead to a significant increase in the average number of scheduled users.

[10]Notice that this is not true for non-LOS channels, whereas it holds true when the spatial scattering is symmetrically distributed around the LOS direction.

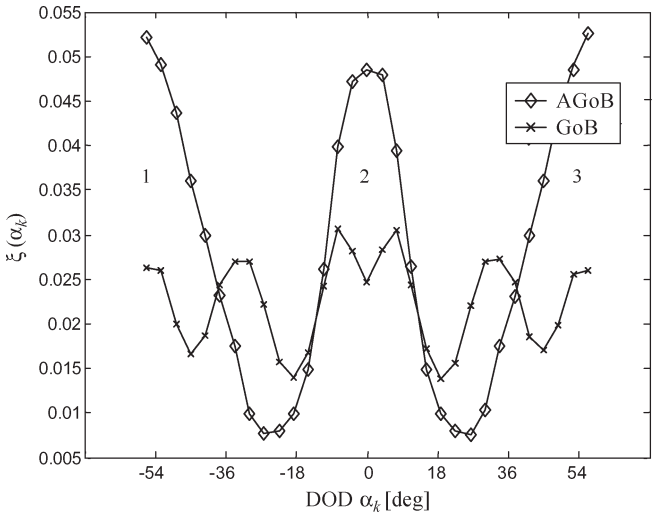

Fig. 11. Probability density function for the angular position α_k of any user k that belongs to the selected user subset S for AGoB and GoB ($L = 7$). The user subset S is constrained to have cardinality M.

To further comment on this aspect, let us consider the following metric:

$$\xi(\alpha_k) \triangleq \Pr(\alpha_k, |\mathcal{S}| = M | k \in \mathcal{S}) = \Pr(\alpha_k | k \in \mathcal{S}, |\mathcal{S}| = M) \cdot p_M \quad (16)$$

which represents the probability density function of the angular position α_k for any user belonging to the selected subset $\mathcal{S}$ with probability p_M (thus, cardinality $|\mathcal{S}| = M$). The metric (16) is chosen to compare the angular distributions of the scheduled users that result from the two spatial multiplexing techniques, under the constraint that the BS is simultaneously serving $M = 3$ users (fully loaded BS). The function $\xi(\alpha_k)$ is used to analyze the coverage capabilities of the proposed techniques. Notice that the distance of the MSs toward the destination is fixed. This is done to highlight the advantages of the adaptive and fixed scheduling schemes rather than the impact of the path loss and/or shadowing on the downlink performances. In Fig. 11, the probability function $\xi(\alpha_k)$ is plotted versus the angular position α_k of the allocated users for both the AGoB and the GoB schemes for $L = 7$. Although for AGoB the probability p_M of serving M users is higher with respect to GoB, the adaptive technique induces clustering of the selected users into M groups to minimize MUI (those groups are indicated as 1, 2, and 3 in Fig. 11 for $M = 3$). On the other hand, the switching phase of the fixed GoB is herein shown to provide more uniform cell coverage compared with AGoB. While, for mobile applications as in the IEEE 802.16-2005 standard [9], [10], this aspect might be less relevant, this is not the case for fixed applications where fixed or nomadic terminals are randomly placed within the cell and are competing for the same time–frequency resource unit.

VII. Concluding Remarks

In this paper, spatial multiplexing techniques for a MIMO–OFDM FDD system have been compared based on varying channel conditions ranging from pure LOS (with a negligible angular spread) to rich scattering (i.e., for a large angular spread). An adaptive technique (AGoB) that enhances the existing GoB scheme has been proposed based on the simultaneous transmission of fixed weighted beams that are adapted to the channel and MUI conditions.

For outdoor environments featuring a moderate angular spread, although the users' subset at the BS is suboptimally designed according to partial CSI in the form of spatial frequencies and SINR lower bounds, AGoB is shown to provide significant benefits compared with the fixed GoB approach. The same time–frequency unit can therefore be scheduled to several users in the same coverage area, leading to a more efficient use of channel resources.

The main conclusions that can be derived from the numerical analysis can be summarized as follows: 1) *Precoder adaptation* in the form of AGoB reveals as a better choice in practice with respect to the *fixed* beam solution (GoB) when outdoor environments exhibit a small angular spread (e.g., $\Phi \leq 25°$); and 2) the additional bandwidth cost (in terms of feedback rate and pilot subcarriers) is negligible, as long as second-order channel statistics (spatial correlations) are slowly varying (as with the spatial frequency).

When environments with richer scattering (larger Φ) are considered, the benefits of precoder adaptation vanish: In that case, since the interference from other in-cell users spreads over the spatial domain, the effectiveness of zero-forcing-based adaptation is significantly reduced, whereas the use of simpler fixed beams for sidelobe suppression still gives valuable improvements.

Finally, the switching phase of the fixed GoB is shown to provide more uniform cell coverage with respect to AGoB. This aspect is mostly relevant in fixed or nomadic applications (see the IEEE 802.16-2004 standard [9], [10]), where each user has to be served with guaranteed quality, regardless of its position in the cell. On the other hand, in mobile applications where users are expected to rapidly cover the whole cell sector, precoder adaptation (as in AGoB) is more effective in that it maximizes the number of users that are simultaneously served.

Appendix A
Spatial Correlation

Under the small angular spread assumption, the spatial correlation can be approximated as a function of the main DOD, so that $\alpha_{n,k} \simeq \alpha_k$, $\forall n$; therefore

$$\mathbf{R}_{T,k} = \sum_{n=1}^{P} \sigma_{k,n}^2 \mathbf{a}_T^*(\alpha_{n,k}) \mathbf{a}_T^T(\alpha_{n,k}) \simeq \mathbf{a}_T^*(\alpha_k) \mathbf{a}_T^T(\alpha_k) \sum_{n=1}^{P} \sigma_{k,n}^2 = \mathbf{a}_T^*(\alpha_k) \mathbf{a}_T^T(\alpha_k). \quad (17)$$

An estimate of α_k, which is herein referred to as $\hat{\alpha}_k$, can easily be obtained by first calculating the spatial correlation. Given F

channel matrix realizations $\mathbf{H}_{k,1},\ldots,\mathbf{H}_{k,F}$, the estimation is obtained as

$$\hat{\mathbf{R}}_{T,k} = F^{-1}\sum_{q=1}^{F}\mathbf{H}_{k,q}^{H}\mathbf{H}_{k,q} \tag{18}$$

by averaging over a number of fading realizations. If uncorrelated fading over each frequency bin can be assumed (the same spatial structure needs to be observed), then the summation in (18) should be performed over the F bins in the frequency domain. For applications where the channel is frequency flat (e.g., fixed or nomadic applications), averaging should instead be obtained over time (e.g., during a specific preamble). By applying (17), the estimation of α_k reduces to the situation described in (9).

Appendix B
Spatial Frequency Estimation

The estimation for the spatial frequency f_k in (9) has to be carried out with no prior information whenever the terminal is turned on. Notice that under the assumption of quantization of $\hat{f}_k$ over b bits, the maximization in (9) requires $\mathcal{O}(N_T^2 2^b)$ flops that can easily be reduced to $\mathcal{O}(N_T-1)2^b)$ by taking into account the symmetric structure of $\mathbf{R}_{T,k}$.

The frequency estimate can be updated frame by frame during each spatial channel allocation phase. A low-complexity algorithm is proposed for the update. The estimate $\hat{f}_{k,\ell}$ for the spatial frequency in the ℓth frame is calculated from the previous frame estimate $\hat{f}_{k,\ell-1}$ and the current channel correlation $\mathbf{R}_{T,k}$ according to

$$\hat{f}_{k,\ell} = \hat{f}_{k,\ell-1} + \mu\frac{\partial}{\partial f}\left|\mathbf{b}^H(f)\mathbf{R}_{T,k}\mathbf{b}(f)\right|_{f=\hat{f}_{k,\ell-1}}. \tag{19}$$

The gradient in (19) is herein approximated by exploiting the Hermitian symmetry of $\mathbf{R}_{T,k}$. It can indeed be shown by tedious, but straightforward, algebraic computations that the following approximation holds:

$$\mathbf{b}^H(f)\mathbf{R}_{T,k}\mathbf{b}(f) \simeq \Gamma_0[\mathbf{R}_{T,k}] + \mathrm{Re}\left[\Omega(\mathbf{R}_{T,k},f)\right] \tag{20}$$

where the term $\Gamma_n[\mathbf{R}_{T,k}] = (1/(N_T-i))\sum_{i=1}^{N_T-i}[\mathbf{R}_{T,k}]_{i,i+n}$ represents the average of the nth diagonal elements of matrix $\mathbf{R}_{T,k}$, whereas $\mathrm{Re}[\Omega(\mathbf{R}_{T,k},f)]$ is the real part of the complex quantity $\Omega(\mathbf{R}_{T,k},f) = (2/N_T)\sum_{n=1}^{N_T-1}\Gamma_n[\mathbf{R}_{T,k}]\exp(-j2\pi f n\Delta_T/\lambda)$. The gradient of (20) can easily be written as

$$\begin{aligned}\frac{\partial}{\partial f}\mathbf{b}^H(f)\mathbf{R}_{T,k}\mathbf{b}(f) &\simeq \frac{\partial}{\partial f}\mathrm{Re}\left[\Omega(\mathbf{R}_{T,k},f)\right]\\ &= \frac{2\pi}{\lambda}\Delta_T\mathrm{Im}\left[\Omega(\mathbf{R}_{T,k},f)\right].\end{aligned} \tag{21}$$

Including the term $2\pi/\lambda\Delta_T$ into the μ quantity, the tracking equation (19) reduces to

$$\hat{f}_{k,\ell} = \hat{f}_{k,\ell-1} + \mu\mathrm{Im}[\Omega(\mathbf{R}_{T,k},\hat{f}_{k,\ell-1})]. \tag{22}$$

With regard to the computation of the step-size μ, notice that if $\hat{f}_{k,\ell-1}$ is near the broadside line, the frequency update is constrained so that $|\hat{f}_{k,\ell}-\hat{f}_{k,\ell-1}| < (3\div 4)\sigma_\alpha$, where σ_α is the standard deviation of the DOD. Slowly varying spatial frequencies might allow the use of only 1 bit of feedback to update the main DOD information. In this case, only the sign of $\hat{f}_{k,\ell}-\hat{f}_{k,\ell-1}$ is significant.

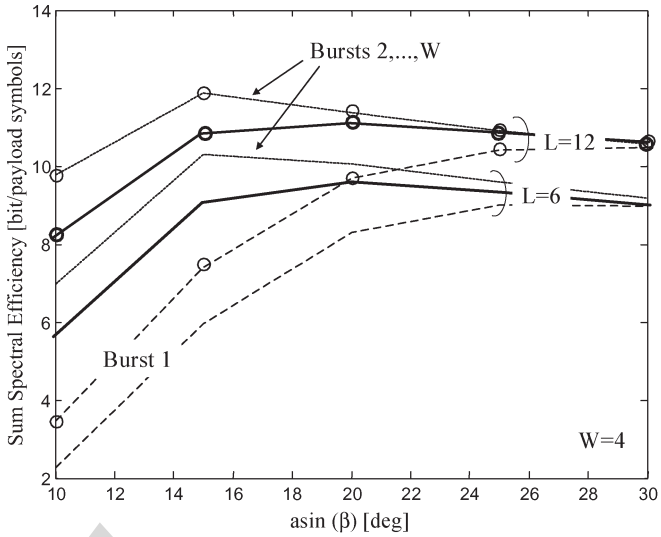

Fig. 12. Average sum spectral efficiency achievable by scheduled users versus β for (no marker) $L=6$ and (circle marker) $L=12$. The sum spectral efficiency is evaluated in (dashed lines) burst 1, (dotted lines) during bursts $2,\ldots,W$, or (solid lines) averaged over the whole frame of $W=4$ bursts. Statistics for angular spreads are the same as for Fig. 5.

Appendix C
Optimization of β

In this paper, the minimum user's spatial separation β is found by maximizing the sum throughput averaged over a number of frames (recall that each frame is composed of W bursts), i.e.,

$$\beta = \arg\max_{\mathcal{S}(\beta)=\{k_1,\ldots,k_M\}} E\left[\frac{1}{W}\sum_{m=1}^{M}\bar{\gamma}(\hat{\rho}_{k_m},\rho_{k_m})\right] \tag{23}$$

where $\bar{\gamma}(\hat{\rho}_{k_m},\rho_{k_m}) = \gamma(\hat{\rho}_{k_m}) + (W-1)\gamma(\rho_{k_m})$, and the expectation is made with respect to the (block) fading that impairs subsequent frames. The SINR indexes k_m refer to users belonging to the selected subset $\mathcal{S}=\mathcal{S}(\beta)=\{k_1,\ldots,k_M\}$ [$\mathcal{S}$ is a function of β from (12)]. Notice that for the kth user, the average throughput within square brackets in (23) is the weighted sum of the spectral efficiency experienced during the first burst of the frame (from worst-case SINR measurements[11] $\hat{\rho}_{k_m}$) and of the spectral efficiency during the remaining $W-1$ bursts (from real SINRs ρ_{k_m}). For propagation settings as in Figs. 6 and 7, we found that $\beta=\sin(20^\circ)$ is the optimal solution (see solid lines in Fig. 12) and holds regardless of the number of active users (as long as L ranges between $L=3$ and $L=12$). The optimal value can be intuitively motivated by noticing that the optimal solution would require the scheduled users to be separated at least by the beampattern mainlobe

[11]Notice that β has a major influence on the worst-case SINRs $\hat{\rho}_{k_m}$ as it constrains the worst-case interference configuration for user k_m.

aperture [34] to minimize interference. As a final remark, we observe that β should be chosen not too large to have a sufficient number of candidate subsets for scheduling; on the contrary, a small value for β would reduce the effectiveness of the worst-case SINR bounds, thus decreasing the sum spectral efficiency for burst 1 (see dashed lines in Fig. 12).

REFERENCES

[1] I. Koutsopoulos and L. Tassiulas, "Adaptive resource allocation in SDMA-based wireless broadband networks with OFDM signaling," in *Proc. IEEE INFOCOM*, Jun. 2002, vol. 3, pp. 1376–1385.

[2] A. Goldsmith *et al.*, "Capacity limits of MIMO channels," *IEEE J. Sel. Areas Commun.*, vol. 21, no. 5, pp. 684–702, Jun. 2003.

[3] Q. H. Spencer, C. B. Peel, L. Swindlehurst, and M. Haardt, "An introduction to the multi-user MIMO downlink," *IEEE Commun. Mag.*, vol. 42, no. 10, pp. 60–67, Oct. 2004.

[4] N. Jindal and A. Goldsmith, "Dirty paper coding vs. TDMA for MIMO broadcast channels," in *Proc. IEEE Int. Conf. Commun.*, Jun. 2004, vol. 2, pp. 682–686.

[5] M. Costa, "Writing on dirty paper," *IEEE Trans. Inf. Theory*, vol. IT-29, no. 3, pp. 439–441, May 1983.

[6] J. Kim and J. Cioffi, "Spatial multiuser access with antenna diversity using singular value decomposition," in *Proc. IEEE Int. Conf. Commun.*, Jun. 2000, vol. 3, pp. 1253–1257.

[7] Q. H. Spencer, A. L. Swindlehurst, and M. Haardt, "Zero-forcing methods for downlink spatial multiplexing in multiuser MIMO channels," *IEEE Trans. Signal Process.*, vol. 52, no. 2, pp. 461–471, Feb. 2004.

[8] D. J. Love and R. W. Heath, Jr., "Limited feedback precoding for spatial multiplexing systems," in *Proc. IEEE Global Telecommun. Conf.*, Dec. 2003, vol. 4, pp. 1857–1861.

[9] *802.16 IEEE Standard for Local and Metropolitan Area Networks Part 16: Air Interface for Fixed Broadband Wireless Access Systems*, IEEE Std. 802.16-2004/Cor1-2005, Sep. 2005.

[10] *802.16 IEEE Standard for Local and Metropolitan Area Networks Part 16: Air Interface for Fixed Broadband Wireless Access Systems*, IEEE Std. 802.16-2005, Feb. 2005.

[11] D. J. Love, R. W. Heath, W. Santipach, and M. Honing, "What is the value of limited feedback for MIMO channels?" *IEEE Commun. Mag.*, vol. 42, no. 10, pp. 54–59, Oct. 2004.

[12] J. Diaz, O. Simeone, and Y. Bar-Ness, "Sum-rate of MIMO broadcast channels with one bit feedback," in *Proc. IEEE Int. Symp. Inf. Theory*, Jul. 2006, pp. 1944–1948.

[13] M. Sharif and B. Hassibi, "On the capacity of MIMO broadcast channels with partial side information," *IEEE Trans. Inf. Theory*, vol. 51, no. 2, pp. 506–522, Feb. 2005.

[14] D. Love, R. Heath, and T. Strohmer, "Grassmannian beamforming for multiple input multiple output wireless systems," *IEEE Trans. Inf. Theory*, vol. 49, no. 10, pp. 2735–2747, Oct. 2003.

[15] K. Mukkavilli, A. Sabharwal, E. Erkip, and B. Aazhang, "On beamforming with finite rate feedback in multiple-antenna systems," *IEEE Trans. Inf. Theory*, vol. 49, no. 10, pp. 2562–2579, Oct. 2003.

[16] R. de Francisco, M. Kountouris, D. T. M. Slock, and D. Gesbert, "Orthogonal linear beamforming in MIMO broadcast channels," in *Proc. IEEE Wireless Commun. Netw. Conf.*, Mar. 11–15, 2007, pp. 1210–1215.

[17] N. Jindal, "MIMO broadcast channels with finite-rate feedback," *IEEE Trans. Inf. Theory*, vol. 52, no. 11, pp. 5045–5060, Nov. 2006.

[18] J. A. C. Bingham, "Multicarrier modulation for data transmission: An idea whose time has come," *IEEE Commun. Mag.*, vol. 28, no. 5, pp. 5–14, May 1990.

[19] T. Yoo and A. Goldsmith, "On the optimality of multiantenna broadcast scheduling using zero-forcing beamforming," *IEEE J. Sel. Areas Commun.*, vol. 24, no. 3, pp. 528–541, Mar. 2006.

[20] T. Yoo, N. Jindal, and A. Goldsmith, "Multi-antenna downlink channels with limited feedback and user selection," *IEEE J. Sel. Areas Commun.*, vol. 25, no. 7, pp. 1478–1491, Sep. 2007.

[21] M. Sternad *et al.*, "Towards systems beyond 3G based on adaptive OFDMA transmission," *Proc. IEEE*, vol. 95, no. 12, pp. 2432–2455, Dec. 2007.

[22] J. Choi and R. W. Heath, Jr., "Interpolation based transmit beamforming for MIMO-OFDM with limited feedback," *IEEE Trans. Signal Process.*, vol. 53, no. 11, pp. 4125–4135, Nov. 2005.

[23] U. Martin, "Spatio-temporal radio channel characteristics in urban macrocells," *Proc. Inst. Electr. Eng.—Radar, Sonar Navig.*, vol. 145, no. 1, pp. 42–49, Feb. 1998.

[24] A. Abdi and M. Kaveh, "A space–time correlation model for multielement antenna systems in mobile fading channels," *IEEE J. Sel. Areas Commun.*, vol. 20, no. 3, pp. 550–560, Apr. 2002.

[25] Y. J. Zhang and K. B. Letaief, "An efficient resource-allocation scheme for spatial multiuser access in MIMO/OFDM systems," *IEEE Trans. Commun.*, vol. 53, no. 1, pp. 107–116, Jan. 2005.

[26] M. Fuchs, G. Del Galdo, and M. Haardt, "A novel tree-based scheduling algorithm for the downlink of multi-user MIMO systems with ZF beamforming," in *Proc. IEEE Int. Conf. Acoust., Speech, Signal Process.*, Mar. 2005, vol. 3, pp. 1121–1124.

[27] EU Integrated Project WINNER Phase I, '*Assessment of advanced beamforming and MIMO technologies,' Deliverable D2.7. 'Assessment of adaptive transmission technologies,' Deliverable D2.4*. [Online]. Available: http://www.ist-winner.org

[28] D. J. Love and R. W. Heath, "Limited feedback diversity techniques for correlated channels," *IEEE Trans. Veh. Technol.*, vol. 55, no. 2, pp. 718–722, Mar. 2006.

[29] H. L. Van Trees, *Optimum Array Processing*. Hoboken, NJ: Wiley, 2002.

[30] M. Wennström, T. Öberg, and A. Rydberg, "Effects of finite weight resolution and calibration errors on the performance of adaptive array antennas," *IEEE Trans. Aerosp. Electron. Syst.*, vol. 37, no. 2, pp. 549–562, Apr. 2001.

[31] W. Wang, T. Ottosson, M. Sternad, A. Ahlén, and A. Svensson, "Impact of multiuser diversity and channel variability on adaptive OFDM," in *Proc. IEEE Veh. Technol. Conf.*, Oct. 2003, vol. 1, pp. 547–551.

[32] W. Weichselberger, M. Herdin, H. Ozcelik, and E. Bonek, "A stochastic MIMO channel model with joint correlation of both link ends," *IEEE Trans. Wireless Commun.*, vol. 5, no. 1, pp. 90–100, Jan. 2006.

[33] T. Park, O. S. Shin, and K. B. Lee, "Proportional fair scheduling for wireless communication with multiple transmit and receive antennas," in *Proc. IEEE Veh. Technol. Conf.*, Oct. 2003, vol. 3, pp. 1573–1577.

[34] U. Spagnolini, "A simplified model to evaluate the probability of error in DS-CDMA systems with adaptive antenna arrays," *IEEE Trans. Wireless Commun.*, vol. 3, no. 2, pp. 578–587, Mar. 2004.

[35] M. Sternad and D. Aronsson, "Channel estimation and prediction for adaptive OFDM downlinks," in *Proc. IEEE Veh. Technol. Conf.*, Oct. 2003, vol. 2, pp. 1283–1287.

[36] M. Cicerone, O. Simeone, and U. Spagnolini, "Channel estimation for MIMO-OFDM systems by modal analysis/filtering," *IEEE Trans. Commun.*, vol. 54, no. 11, pp. 2062–2074, Nov. 2006.

[37] T. Ottosson, M. Sternad, A. Ahlén, and A. Svensson, "Attaining both coverage and high spectral efficiency with adaptive OFDM downlinks," in *Proc. IEEE Veh. Technol. Conf.*, Oct. 2003, vol. 4, pp. 2486–2490.

Stefano Savazzi (S'05) received the M.Sc. and Ph.D. degrees (both with honors) in telecommunication engineering from the Politecnico di Milano, Milano, Italy, in 2004 and 2008, respectively.

He was a Visiting Researcher with the Signals and Systems Laboratory, Department of Engineering Sciences, Uppsala University, Uppsala, Sweden, in 2005 and with Department of Electrical and Computer Engineering, University of California San Diego, in 2007. He is currently with the Dipartimento di Elettronica e Informazione, Politecnico di Milano. He holds a patent on the work developed for his M.S. thesis. His current research interests include signal processing aspects for digital wireless communications and, more specifically, channel estimation, antenna array processing for MIMO-OFDM systems, and cooperative networking.

Monica Nicoli (M'99) received the M.Sc. (with honors) and Ph.D. degrees in telecommunication engineering from the Politecnico di Milano, Milano, Italy, in 1998 and 2002, respectively.

During 2001, she was a Visiting Researcher with the Signals and Systems Laboratory, Uppsala University, Uppsala, Sweden. Since 2002, she has been an Assistant Professor with the Dipartimento di Elettronica e Informazione, Politecnico di Milano. Her research interests are in the area of signal processing for communication systems, including multiuser/multiantenna/multicarrier systems, radio localization, cooperative communications and distributed processing in wireless sensor networks.

Dr. Nicoli was a recipient of the Marisa Bellisario Award in 1999.

Mikael Sternad (S'83–M'88–SM'90) was born in Eskilstuna, Sweden, in 1957. He received the Ph.D. degree in automatic control from Uppsala University, Uppsala, Sweden, in 1987.

He is currently a Professor of automatic control with the Signals and Systems Laboratory, Department of Engineering Sciences, Uppsala University. Since 2000, he has been the Leader of the Wireless IP project, which is a collaboration between Uppsala University, Chalmers University of Technology, Göteborg, Sweden, and Karlstad University, Karlstad, Sweden, on 4G wireless systems based on adaptive techniques. He has been active within the EU WINNER projects, working on channel prediction, adaptive transmission, deployment techniques, multiple access, and overall system design, leading work on MAC layer design. Having authored around 110 papers and five book chapters and with a background in robust and adaptive estimation, control, and filtering, his main current research interests are the many tradeoffs and design issues encountered in wireless systems design and the use of signal processing and control algorithms in communication systems. He is also involved in acoustic signal processing, particularly precompensation of room acoustics and car audio systems. He is a cofounder and was the Chairman of the Board (2001–2005) of Dirac Research, i.e., a company working in this field.